



Uterine mesenchymal tumors: development and preliminary results of a magnetic resonance imaging (MRI) diagnostic algorithm

Francesca Rosa¹ · Carola Martinetti² · Silvia Magnaldi³ · Stefania Rizzo^{4,5} · Lucia Manganaro⁶ · Stefania Migone² · Silvia Ardoino⁷ · Daria Schettini² · Pierangelo Marchiolè^{8,9} · Tommaso Ragusa¹⁰ · Nicoletta Gandolfo²

Received: 23 February 2023 / Accepted: 25 May 2023 / Published online: 14 June 2023
© Italian Society of Medical Radiology 2023

Abstract

Purpose The aim of our study is to propose a diagnostic algorithm to guide MRI findings interpretation and malignancy risk stratification of uterine mesenchymal masses with a multiparametric step-by-step approach.

Methods A non-interventional retrospective multicenter study was performed: Preoperative MRI of 54 uterine masses was retrospectively evaluated.

Firstly, the performance of MRI with monoparametric and multiparametric approach was assessed. Reference standard for final diagnosis was surgical pathologic result ($n = 53$ patients) or at least 1-year MR imaging follow-up ($n = 1$ patient).

Subsequently, a diagnostic algorithm was developed for MR interpretation, resulting in a Likert score from 1 to 5 predicting risk of malignancy of the uterine lesion. The accuracy and reproducibility of the MRI scoring system were then tested: 26 preoperative pelvic MRI were double-blind evaluated by a senior (SR) and junior radiologist (JR).

Diagnostic performances and the agreement between the two readers with and without the application of the proposed algorithm were compared, using histological results as standard reference.

Results Multiparametric approach showed the best diagnostic performance in terms of accuracy (94.44%), and specificity (97.56%).

DWI was confirmed as the most sensible parameter with a relative high specificity: low ADC values (mean 0.66) significantly correlated to uterine sarcomas diagnosis ($p < 0.01$).

Proposed algorithm allowed to improve both JR and SR performance (algorithm-aided accuracy 88.46% and 96%, respectively) and determined a significant increase in inter-observer agreement, helping even the less-experienced radiologist in this difficult differential diagnosis.

Conclusions Uterine leiomyomas and sarcomas often show an overlap of clinical and imaging features.

The application of a diagnostic algorithm can help radiologists to standardize their approach to a complex myometrial mass and to easily identify suspicious MRI features favoring malignancy.

Keywords Leiomyoma · Uterine sarcoma · Magnetic resonance imaging · Diffusion-weighted imaging · Diagnostic algorithm

Abbreviations

MRI Magnetic resonance imaging
LMS Leiomyosarcomas
LG ESS Low-grade endometrial stromal sarcoma
HG ESS High-grade endometrial stromal sarcoma
US Undifferentiated sarcoma
AD Adenosarcoma

STUMP Smooth muscle tumor of uncertain malignant potential
ESUR European Society of Urogenital Radiology
WI Weighted imaging
FS Fat suppression
DWI Diffusion-weighted imaging
ADC Apparent diffusion coefficient
SR Senior radiologist
SI Signal intensity
CE Contrast enhancement
ROI Region of interest
JR Junior radiologist

F. Rosa and C. Martinetti have contributed equally to this work.

Extended author information available on the last page of the article

ROC	Receiver operating characteristic
CI	Confidence intervals
PPV	Positive predictive value
NPV	Negative predictive value
FN	False negative
FP	False positive

Introduction

Uterine leiomyomas are benign mesenchymal tumors that arise from myometrial smooth muscle cells and represent the most frequent benign tumors of the uterus (up to 20–40% of women of reproductive age and 70–80% of peri-menopausal women) [1, 2].

The histological classification includes typical, degenerated leiomyomas and several subtypes such as cellular leiomyoma, lipoleiomyoma and leiomyoma with bizarre nuclei.

On the other hand, uterine sarcomas are a heterogeneous group of rare neoplasms originating from the myometrium or from endometrial mesenchymal tissue and represent less than 10% of tumors occurring in uterus body [3]. Although rare, uterine sarcomas represent the most aggressive malignant uterine tumors, showing rapid growth and dissemination with a 5-year survival rate ranging between 17.5 and 54.7% [4].

Uterine sarcomas include leiomyosarcoma (LMS), low and high grade endometrial stromal sarcoma (LG-ESS, HG-ESS), undifferentiated uterine sarcoma (US), and adenosarcoma (ADS) [5].

The term STUMP (Smooth-muscle Tumors of Uncertain Malignant Potential) refers to another subtype of myometrial lesions, originating from uterine smooth muscle cells that cannot be diagnosed unequivocally as benign or malignant, also histologically.

Clinical manifestations of uterine sarcomas and leiomyomas can be similar including a rapidly increasing size mass, abdominal pain, and vaginal bleeding.

The differential diagnosis of these two entities is challenging but a correct preoperative risk stratification is crucial to avoid inappropriate management.

The therapeutic options for typical leiomyoma include conservative/mini-invasive; meanwhile, uterine sarcoma requires a more aggressive treatment (extensive surgery with hysterectomy and bilateral salpingo-oophorectomy is considered the treatment of choice) [6, 7].

In this clinical context, the imaging could play a pivotal role and MRI is considered one of the best tools for myometrial masses characterization [8].

However, MRI differential diagnosis remains challenge due to the overlap of imaging features between sarcomas and leiomyomas especially if atypical, large, or degenerated ones [9, 10].

Several studies since 2008 tried to propose imaging-based methods to distinguish these two entities. It is important to note that almost all studies published are retrospective and with a small cohort of patients (the number ranged from 9 to 19); there is only one prospective study but with a cohort of only 6 cases of uterine sarcoma and 25 benign lesions [11].

The aim of our study is to propose a diagnostic algorithm to guide MRI findings interpretation and to allow malignancy risk stratification of uterine masses through a multiparametric step-by-step approach.

Materials and methods

This non-interventional, observational, and retrospective study was in accordance with the ethical standards of the institutional and national research committee and with the 1964 Helsinki Declaration. It is approved by the Regional Ethics Committee (N. CER Liguria: 78/2023-DB id 12,883). Informed consent was obtained from participants included in the study.

Patients

We retrospectively queried our database from January 2015 to April 2023 and selected patients with clinical suspicion of malignant mesenchymal tumor.

The inclusion criteria were clinical and radiological suspicion of uterine mesenchymal tumor, preoperative pelvic MR examination with adequate protocol (details in next paragraph) and a confirmed histopathological diagnosis of uterine leiomyomas or sarcomas or MRI follow-up for at least 1 year in the absence of surgery.

We excluded patients who underwent MR examinations with incomplete protocols and cases of carcinosarcoma which *is no longer classified as a sarcoma but as a high-risk variant of endometrial carcinoma*.

Overall design of study

The investigation was divided into two parts:

Firstly, based on literature data, we selected morphological and functional MRI features already demonstrated useful for the characterization of mesenchymal uterine masses [11–19], as given in Table 1.

An initial cohort, called training set, included 54 uterine mass was used to assess the performance of previously validated MR parameters evaluating both mono-parametric and multiparametric approach.

Then, we construct an MR imaging diagnostic algorithm and scoring system based on previous study results [11–26].

Table 1 Imaging features and lexicon for a morphologic and functional evaluation of uterine lesions based on literature data [11–23]

MR parameter	Definition	Features favoring <i>benignity</i>	Features favoring <i>malignancy</i>	Pitfalls
DWI Signal	<ul style="list-style-type: none"> - <i>Restricted DWI</i>: DWI hyperintensity comparing with SI outer myometrium on the high b value. ADC hypointensity ($< 1.05 \times 10^{-3} \text{ mm}^2/\text{sec}$) - <i>No restricted DWI</i>: DWI hypointensity on the high b value. ADC hyperintensity ($> 1.05 \times 10^{-3} \text{ mm}^2/\text{sec}$) 	No restricted DWI	Restricted DWI	<ul style="list-style-type: none"> - Artifacts due to blood products: correlation with T1wi FS (hyperintense areas) is mandatory - Measure ADC value only for confirmation avoiding necrotic/cystic areas, by looking at T1 and T2wi - <i>T2 blackout effect</i>: collagen deposition decreases SI both on DWI and ADC map
T2 WI signal	<ul style="list-style-type: none"> - Homogeneous - Heterogeneous - Hypo/hyperintense compared to the adjacent external myometrium - Cystic degeneration: well-defined areas with high T2 SI (with low T1 SI) 	Homogeneous and Hypointense T2 SI	Heterogeneous and Intermediate T2 SI	<ul style="list-style-type: none"> -T2-hyperintense rim indicates periwound oedema around large lesions: not to consider in the characterization of intralesional signal -T2 homogeneous slightly hyperintense signal could occur as the first sign of degeneration in a leiomyoma → look at DWI (No restricted) and C.E
T1 FS WI Signal	-Haemorrhagic intralesional areas defined as areas of T1 hyperintensity in the Fat Sat images (periph-eric, diffuse or central)	Absence of Haemorrhagic areas	Central Haemorrhagic areas	<ul style="list-style-type: none"> -<i>Red degeneration</i>: peripheral haemorrhagic rim/diffuse T1 hyperintensity (venous infarction and coagulative necrosis) →check internal margins (smooth) and correlate with patient history and symptoms (pain, hormonal insult, systemic upset such as fever and leucocytosis) -<i>Uterine sarcomas</i>: intralesional central hemorrhagic foci (tumoral hemorrhagic necrosis) - <i>Lipoleiomyoma</i>: intralesional fat has high signal on T1WI but hypointense (suppressed) SI on fat-suppressed imaging

Table 1 (continued)

MR parameter	Definition	Features favoring benignity	Features favoring malignancy	Pitfalls
Contrast Enhancement (C.E.)	<ul style="list-style-type: none"> - No C.E. (completely avascular lesion) - Homogeneous and late C.E. compared to myometrium - Heterogeneous C.E. in early/arterial phase compared to myometrium - Intralesional necrosis defined as irregular, often central, areas of lacking C.E. at venous and later phases 	Completely avascular Or Homogeneous C.E.	Heterogeneous early/arterial C.E. and/or Central area of necrosis	<ul style="list-style-type: none"> - <i>Degenerated leiomyomas</i> with inter-nal avascular areas corresponding to cystic/hyaline or red cell degeneration →check signal on T2- and T1-wi and inner margins - <i>Cellular leiomyomas</i> can show early but homogeneous and restricted diffusion
Border	Defined regular/irregular or poor defined	Regular	Irregular or infiltrative	

In a second step, the accuracy and reproducibility of the MR imaging algorithm and scoring system were tested in 26 uterine masses (this set was called internal validating set).

MRI protocol

All MRIs were performed with a commercially available 1.5 T systems (Inginia®, Philips Healthcare, Netherlands; Magnetom Aera®, Siemens Healthcare, Germany) using a phased array pelvic coil.

According to European Society of Urogenital Radiology (ESUR) recommendations [11], pelvic MR studies were considered adequate if consisted of at least (detailed protocol is shown in Supplemental material 1):

- T2-weighted images (WI), for morphological evaluation of the pelvis, in at least two orthogonal planes, one of which sagittal.
- T1-WI in the axial plane with and without fat suppression (FS) before contrast administration.
- Diffusion-weighted images (DWI), in the axial plane with a minimum of two b values, respectively, low (50 s/mm²) and high (800–1000 s/mm²) with apparent diffusion coefficient (ADC) map.
- Post-contrast T1-WI acquisition with gradient-echo, fat-suppressed sequence acquired at least with a multiphasic technique (T1vibedixon) consisting of an early post-contrast phase (30–60 s), equilibrium phase (120–180 s) and delayed phase (4–5 min). A bolus injection of 0.2 mL/kg of gadoteric acid at an injection rate of 2 mL/sec followed by a 25-mL saline flush given through a power injector (Medrad®, Bayer).

Before each MR examination, specific clinical information was collected (menstrual cycle status, symptoms, any hormonal therapy, previous abdominal-pelvic interventions).

Data analysis

Clinical and pathologic data were collected including size and histologic type of the lesions.

Firstly, mono-parametric and multiparametric MRI performance in the diagnosis of uterine sarcomas was evaluated in our cohort (a total of 54 uterine mass) and the final diagnoses were confirmed by pathologic examination ($n = 53$ patients) and/or by at least 1-year of MR imaging follow-up ($n = 1$ patient).

MR examinations were evaluated by a senior radiologist (SR, SM) with 8 years of experience in gynecological imaging who was blinded to pathology.

According to previous studies, we selected all MRI features that had to be evaluated and considered useful for mesenchymal mass differential diagnosis and defined a proper

lexicon for uterine lesions description [11–19], as given in Table 1.

The following MRI features were evaluated:

- (a) *T2 signal intensity (SI)* was compared with the adjacent external myometrium.

A low signal intensity was defined as lower or equal to signal of the external myometrium, an intermediate signal intensity as higher than that the myometrium; a high T2 SI was defined as equal to fluid component signal (such as cerebrospinal fluid).

Well-defined areas with high T2 SI (and corresponding low T1 SI) were defined as areas of cystic degeneration. These could be associated with a thin low T2 SI rim with contrast enhancement (C.E.), representing non degenerated tissue.

Homogeneity of T2 SI was also assessed in two categories (homogeneous and heterogeneous).

- (b) *DWI SI* was visual assessed comparing SI on the high B-value (b 1000) of the lesion with the signal of the outer myometrium. The presence of restricted diffusion is defined by DWI hyperintensity (comparing with SI of the endometrium) associated to ADC hypointensity.

ADC values of each tumour were also measured positioning a region of interest (ROI) on the ADC map in the area with the lowest signal, avoiding haemorrhagic, necrotic, or cystic portions.

Several regions of interest (ROI) were placed on the maps, and the lowest value of mean ADC was recorded.

- (c) *T1-WI SI*

was evaluated to demonstrate presence/absence of intralesional fat or hemorrhagic foci. Hemorrhagic foci corresponded to hyperintense intralesional areas on T1-FS images before contrast and can look like a

peripheric hemorrhagic rim (typical for red degeneration) or intralesional central hemorrhagic foci (favoring sarcoma hypothesis), as shown in Figs. 1 and 2.

- (d) *Contrast enhancement on T1wi*

Homogeneous vascularization or completely avascular lesion with a regular internal profile is considered associated to benign lesions.

The presence of early inhomogeneous enhancement, presence of necrosis at equilibrium and delayed phases, homogeneous contrast enhancement or completely avascular lesion with smooth inner margin had to be described [12, 13], as shown in Figs. 1 and 2.

Early inhomogeneous enhancement and/or the presence of necrosis at venous phase and later phases were considered features favoring malignancy.

Necrosis is defined as irregular, often central, focal areas of lacking C.E. at equilibrium and delayed phases that no correspond to area of cystic degeneration (high signal on T2).

- (e) *Morphological features* dimensions (largest diameter of the lesion regardless of the plane) and the type of border (regular versus irregular/infiltrative) were described.

- (f) The presence of ascites (fluid extended above uterine fundus), peritoneal pelvic implants (nodular or diffuse thickening of anterior and/or posterior pelvic peritoneal reflection, Supplemental material and 2) extraperitoneal implants (e.g., mesorectum), pelvic lymphadenomegalies (short axis > 10 mm) and infiltration of adjacent structures.

As second step of our study, a diagnostic algorithm was developed for MR signal interpretation adopting a proper lexicon based on literature data (Fig. 3).

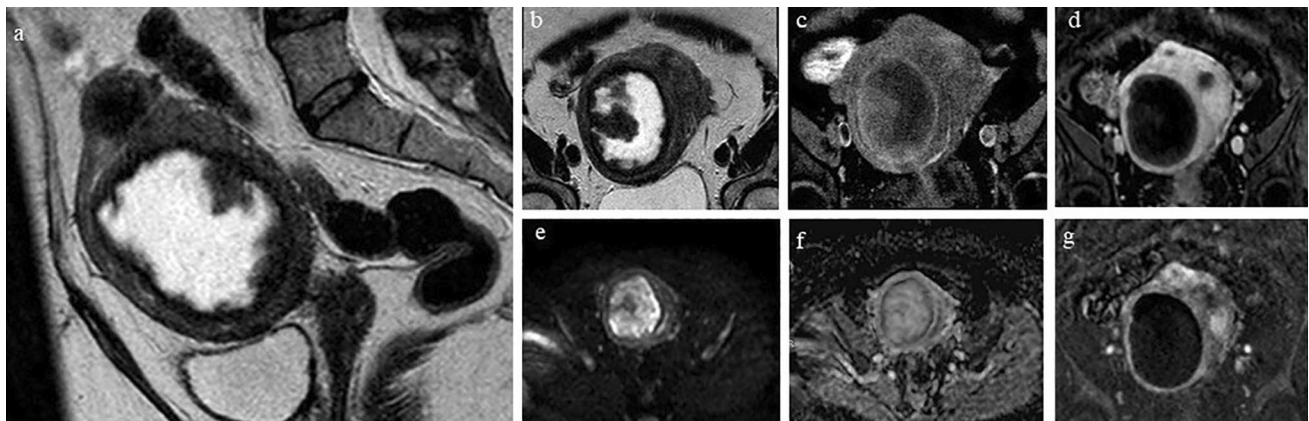


Fig. 1 Red degeneration of uterine leiomyoma: sagittal (a) and axial (b) T2WI showed an uterine lesion with smooth margins and an internal T2 hyperintense area with a peripheric internal rim slightly hyperintense on T1FS WI, compatible with hemorrhagic degenera-

tion (c); the lesion showed no restricted diffusion on DWI and ADC map (e) and (f); post-contrast T1WI (d) showed a complete absence of contrast enhancement of the lesion with smooth and regular internal margins confirmed also by subtraction images (g)

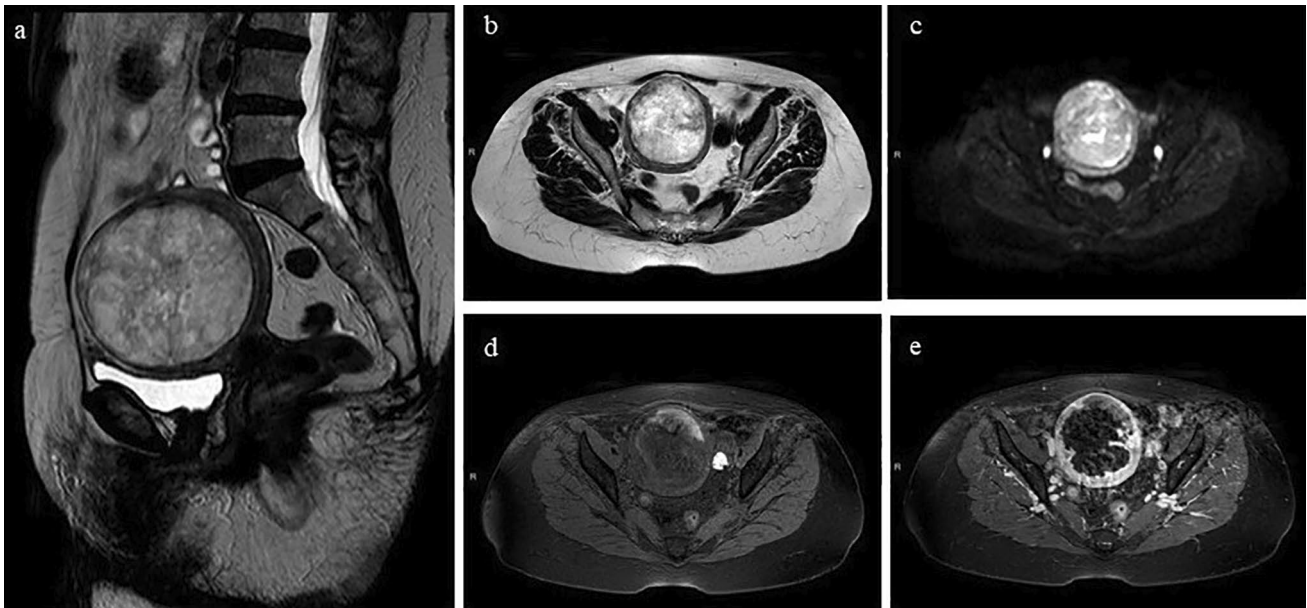


Fig. 2 Uterine adenocarcinoma: sagittal **a** and axial **b** T2WI showed a heterogeneous hyperintense uterine lesion with smooth margins; the lesion was characterized by restricted diffusion on DWI **c**. T1FS WI

d showed internal focal and eccentric hemorrhagic foci and T1FS WI after contrast injection **e** demonstrated internal areas of necrosis with irregular internal margin

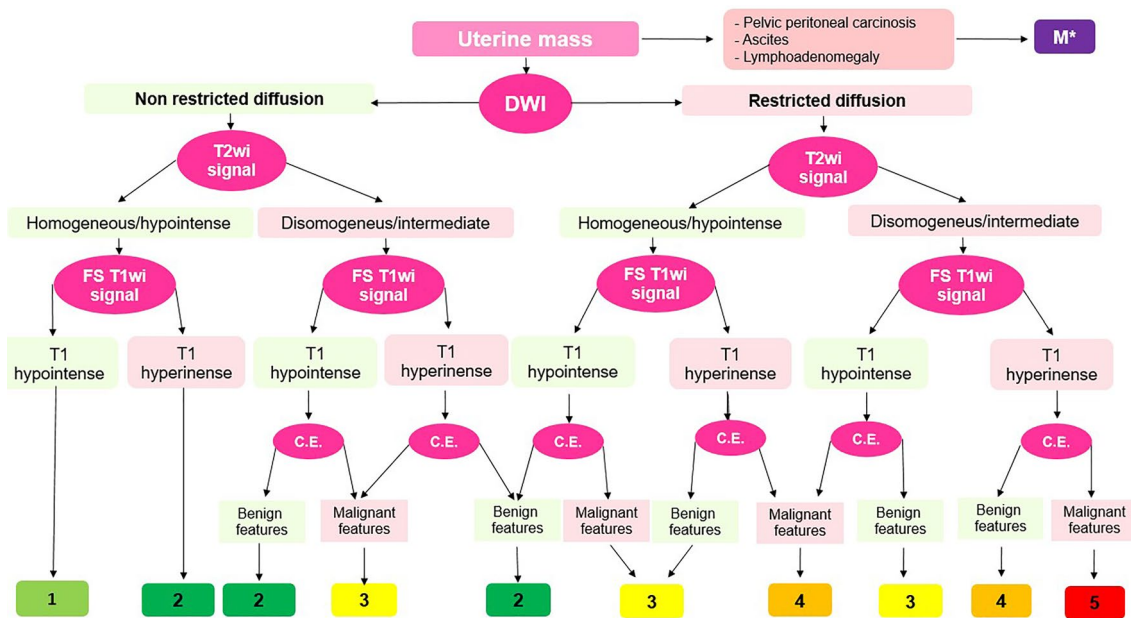


Fig. 3 Proposed MRI diagnostic algorithm. M* = signs of malignancy but not specific of uterine sarcoma

The result of the diagnostic algorithm is a Likert score from 1 to 5 predicting risk of malignancy of the uterine lesion, in particular:

- *Score 1*: benign lesion
- *Score 2*: probably benign lesion
- *Score 3*: indeterminate lesion (low risk of uterine sarcoma)
- *Score 4*: probably malignant lesion (high risk of uterine sarcoma)
- *Score 5*: high suspicious malignant lesion (very high risk of uterine sarcoma)

– *Score M*: malignant lesion but not specific for Uterine sarcoma.

In our algorithm, DWI, T2, T1 signal and type of contrast enhancement are considered as major features to be evaluated.

Meanwhile type of margins and biological behavior (rapid growth lesions in a post-menopausal woman) are considered as ancillary features.

Ascites, peritoneal pelvic implants and lymph adenomegalies are considered independently as signs of malignancy but not specific of uterine sarcoma.

Aware of the limit given by dependence of ADC values by the different machines, for quantitative ADC map interpretation (useful especially on visual assessment doubt case) we used a cutoff of $1.05 \times 10^{-3} \text{ mm}^2 \text{ s}^{-1}$ based on literature data [27].

Only in the case of a score of 3 (indeterminate lesion), the algorithm required the evaluation of ancillary features. The presence of at least one of these features (lesion with irregular margins, rapid growth of uterine mass in a perimenopausal/menopausal woman) allowed to attribute a score of 4 to a lesion previously assessed as indeterminate based on MRI signal, as shown in Fig. 4.

The presence of signs of ascites associated with pelvic peritoneal or extraperitoneal implants and pelvic pathological lymphadenomegalies was considered as independent characteristics that allowed the patient to be framed in a different category likely malignant (“M”), not specific for uterine sarcoma.

The accuracy and reproducibility of the MR imaging scoring system were tested: 26/54 preoperative pelvic MR examination of the training set were double blind evaluated by a SR (N.G.) with 10 years of experience in gynecological imaging and by a Junior Radiologist (JR, C.M.) with 3 years of experience in Gynecological Imaging).

The first read was performed without knowing the diagnostic algorithm.

The second read (algorithm-aided report) was performed after an explanation of the proper lexicon and the definition of each imaging features included in the algorithm.

Diagnostic performances and the agreement between the two readers with and without the application of the proposed algorithm were compared.

Diagnostic performances were compared using histological results as standard reference.

Reference standard

Final diagnoses were established by surgical pathologic results for 53 lesions and based on 1-year MR imaging follow-up for 1 lesion.

Statistical analysis

Statistical analysis was performed using Microsoft Excel and MedCalc® Statistical Software.

Diagnostic performance of each MR parameter (DWI, T2 SI, T1 SI, post-contrast T1 enhancement) and of MR with a multiparametric approach were evaluated in terms of sensitivity, specificity, positive/negative likelihood ratio, positive/negative predictive value, accuracy.

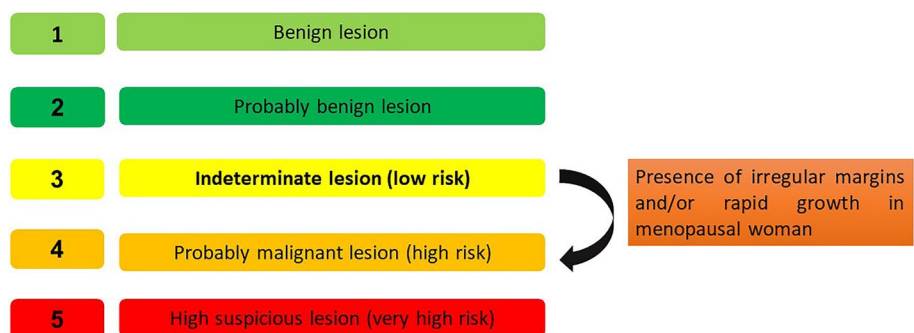
Receiver operating characteristic (ROC) analysis was performed to determine cutoff and diagnostic performance for ADC value.

Two tailed Fischer’s exact test was used, considering the few values in the contingency table, to determine significance association between clinical and imaging features. Probability (*p*) values < 0.05 were considered significant.

We compared SR and JR performance (algorithm-aided and non-algorithm-aided report) in terms of accuracy, sensitivity, specificity, and 95% confidence intervals (CIs) of each parameter.

The Cohen’s kappa coefficient after dichotomization of Likert scales (cutoff > 3) was calculated to evaluate the agreement between SR and JR before and after the application of the proposed algorithm: Scales of 4 and 5 were regarded positive, whereas scales of 1–3 negative.

Fig. 4 Ancillary features: in the case of a score of 3 (indeterminate lesion), the presence of at least one of these features (lesion with irregular margins, rapid growth of uterine mass in a perimenopausal/menopausal woman) allowed to attribute a score of 4 to a lesion previously assessed as 3



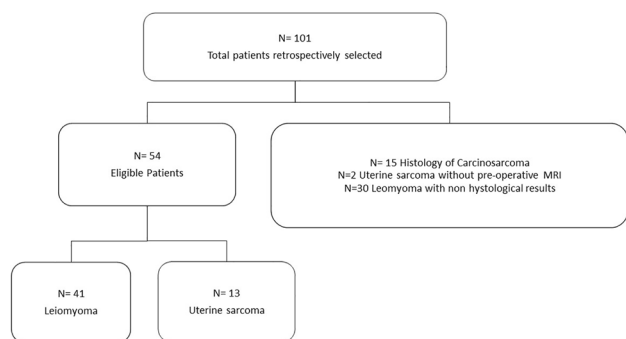


Fig. 5 Study flowchart

Results

Fifty-four MR examinations of patients meeting the inclusion criteria were retrospectively reviewed as training set: 41/54 were found with histological diagnosis of uterine leiomyoma and 13/54 with histological diagnosis of uterine sarcoma (7 LMS, 1 STUMP, 1 LG-ESS, 3 HG-ESS and 1 AS). Study population is shown in Fig. 5.

The average age of the patients examined was 54 years (range 36–84), with an average age of 53 years for patients with uterine sarcoma and 54 years for patients with leiomyoma.

We found no significant correlation between lesion dimension and the number (single versus multiple lesions).

The diagnostic performances of each MRI parameters and of MRI with a multiparametric approach were shown in the Table 2: data confirmed the superiority of a multiparametric approach (at least 3 MRI parameters) to obtain the best diagnostic accuracy.

DWI was confirmed as the most sensible parameter with a relative high specificity, as demonstrated in previous works [16, 17]: low ADC values (mean 0.66) significantly correlated to uterine sarcomas diagnosis ($p < 0.01$), as shown in Fig. 6.

The internal validation set was a cohort of 26 uterine mass: 14/26 were found with histological diagnosis of uterine leiomyoma (5 typical leiomyoma, 3 red degenerated, 4 myxoid degenerated, 1 cellular leiomyoma and 1 leiomyoma with bizarre nuclei) and 12/26 with histological diagnosis of uterine sarcoma (7 LMS, 1 STUMP, 1 LG-ESS, 2 HG-ESS and 1 AS).

The JR and SR performance in terms of sensitivity, specificity, positive and negative likelihood ratio for algorithm-aided and not algorithm-aided diagnosis of uterine sarcoma is shown in the Table 3.

Both readers improved their performance adopting the proposed diagnostic algorithm.

The JR algorithm-aided performance in terms of sensitivity, specificity, positive predictive value (PPV), negative predictive value (NPV), and accuracy was, respectively, 100.00%, 78.57%, 80.00%, 100.00% and 88.46%.

SR increased the performance too obtaining a sensitivity, specificity, PPV, NPV, and accuracy, respectively, of 100.00%, 93.33%, 92.31%, 100.00% and 96.30%.

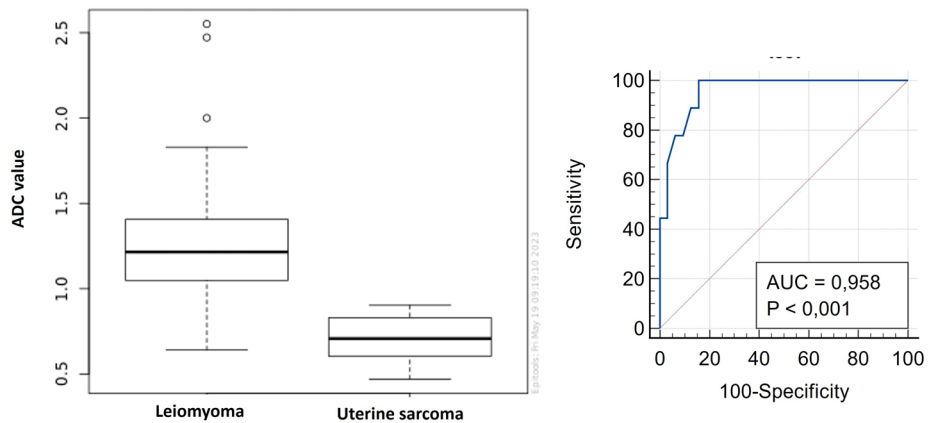
The inter-readers agreement has been evaluated by considering the following scale of values for the interpretation of the Cohen's k values:

- < 0 : No agreement
- 0.00–0.20: slight agreement
- 0.21–0.40: fair agreement
- 0.41–0.60: moderate agreement
- 0.61–0.80: substantial agreement

Table 2 Diagnostic performances of each MRI parameters and the multiparametric approach

	Sensitivity (95% CIs)	Specificity	<i>P</i> -value	PPV (%)	NPV (%)	Accuracy (%)
DWI	100% (75.29% to 100.00%)	82.93% (67.94% to 92.85%)	< 0.01	65	100	87
T2 SI	100% (75.29% to 100.00%)	36.59% (22.12% to 53.06%)	< 0.05	33.33	100%	51.85
T1 SI	69.23% (38.57% to 90.91%)	87.8% (73.80% to 95.92%)	< 0.01	64.29	90	83.33
Post-contrast T1 enhancement	53.85% (25.13% to 80.78%)	87.8% (73.80% to 95.92%)	< 0.05	58.33	85.71	79.63
Multiparametric approach (3 features)	84.62 (54.55% to 98.08%)	97.56% (87.14% to 99.94%)	< 0.01	91.67	95.24	94.44
Multiparametric approach (4 features)	38.46% (13.86% to 68.42%)	100% (91.40% to 100.00%)	< 0.01	100	83.67	85.19
Border	53.8% (25.13% to 80.78%)	95% (83.08% to 99.39%)	< 0.01	77.78	86.36	78.9

Fig. 6 Box and whisker plots representing ADC values in uterine leiomyomas and sarcomas (on the left). ROC curve shows the diagnostic performance of ADC values in differentiating leiomyomas from uterine sarcomas. ADC values distribution are also shown in the table



	Min	Median	Max	Mean	SD
Leiomyoma	0,641	1,22	2,55	1,3	0,435
Uterine sarcomas	0.47	0.66	0.903	0.686	0.1547

– 0.81–1.00: near perfect agreement

We observed:

- A moderate agreement (Cohen’s k: 0.571) between SR and JR without the use of the diagnostic algorithm.
- Near perfect agreement (Cohen’s k: 0.847) between SR and JR’s algorithm-aided report.

Table 3 JR and SR performance for algorithm-aided and not algorithm-aided diagnosis of uterine sarcoma

Statistical analysis	Value	95% CI
<i>Junior reader without algorithm</i>		
Sensitivity	75.00%	19.41% to 99.37%
Specificity	68.75%	41.34% to 88.98%
Positive Likelihood Ratio	2.40	0.96 to 6.03
Negative Likelihood Ratio	0.36	0.06 to 2.05
<i>Junior reader algorithm-aided diagnosis</i>		
Sensitivity	100%	73.54% to 100%
Specificity	78.57%	44.20% to 95.34%
Positive Likelihood Ratio	4.67	1.71 to 12.72
Negative Likelihood Ratio	0	0
<i>Senior reader without algorithm</i>		
Sensitivity	80.00%	28.36% to 99.49%
Specificity	73.33%	44.90% to 92.21%
Positive likelihood ratio	3.00	1.16 to 7.73
Negative likelihood ratio	0.27	0.05 to 1.62
<i>Senior reader algorithm-aided diagnosis</i>		
Sensitivity	100.00%	73.54% to 100.00%
Specificity	93.33%	68.05% to 99.83%
Positive likelihood ratio	15.00	2.26 to 99.64
Negative likelihood ratio	0.00	0

Discussion

Historically, uterine sarcomas are considered a rare clinical entity with reported prevalence of LMS (the most frequent subtype) ranged between 0.003 and 0.007% but presently the true prevalence is estimated to be between 0.2 and 0.4% [18].

The preoperative diagnosis of uterine sarcomas has important clinical, therapeutic as well as prognostic values.

In this scenario, several studies try to find clinical, radiological or laboratoristic parameters able to provide an adequate preoperative malignancy risk assessment of myometrial lesions.

The role of MR imaging is a current and still debated argument, although MR is considered the best imaging modality for characterization and staging of uterine masses.

The diagnostic accuracy of each individual MR parameters in the diagnosis of uterine sarcomas was evaluated by several studies but it is demonstrated that there is frequently an overlap of MR features between uterine LM and sarcoma.

In 2008, Tamai et al. [17] published a paper proposing the use of DWI and the corresponding ADC map to distinguish sarcomas and cellulated leiomyomas from typical and/or degenerate leiomyomas. However, they found an overlap of DWI and ADC values between typical leiomyomas, cellulated leiomyomas and uterine sarcomas.

In 2009, Namimoto et al. [19] tried to increase MR diagnostic accuracy by combining tumor ADC values with the T2 SI: They obtained a sensitivity and specificity of 100% in the diagnosis of sarcoma.

Other authors proposed a multiparametric approach as, in 2013, Thomassin-Naggara et al. [20] who demonstrated how sarcoma can be diagnosed with an accuracy of 92.4%

through the combination of age (> 44 years old), T2 and DWI SI but they didn't consider T1 signal and the type of contrast enhancement.

In 2015, Lin et al. [21] prospectively investigated the added value of contrast media: They demonstrated how the combination of DWI and ADC values achieved equivalent accuracy than the use of contrast media in the diagnosis of uterine sarcoma. T2 signal and presence of hemorrhagic foci were not evaluated.

In 2018, the systematic review published by Kaganov et al. [22] found no significant associations between ADC values and sarcoma diagnosis, while it demonstrated that the combination of T1 and T2 signal is more effective and contributed to the diagnosis of sarcoma with a specificity of 77.78%.

To increase sensitivity and specificity in the distinction between uterine sarcomas and leiomyomas, Nagai et al. [23] proposed to combine clinical and radiological data and elaborated a preoperative score for the evaluation of uterine sarcomas. Four features had to be evaluated: age at surgery, serum lactate-dehydrogenase level, MRI findings (T1 hyperintensity and/or T2 heterogeneous signal) and cytology results. However, neither DWI signal nor post-contrast sequences have been used in this work.

Presently, there is no agreement in literature about what MR parameters is the most sensitive and specific for malignant myometrial lesion detection. The most important imaging features for this difficult differential diagnosis and the most representative research about this argument have been recently reviewed by Sun et al. and Smith et al. [24, 25].

The aim of our study was to propose a diagnostic algorithm for the differential diagnosis between uterine sarcomas and leiomyomas evaluating all MRI features described in literature already validated for uterine sarcoma diagnosis. We decided to not include texture analysis because it is a less reproducibly technique especially for less subspecialized readers.

In our paper, firstly we evaluated the performance of previously validated MR parameters on our cohort of patients.

All signal MR features described in literature as predictive of malignancy (T2 intermediate signal, DWI/ADC restricted signal, areas of hemorrhage on T1WI and early enhancement and central areas of necrosis on post-contrast sequence) significantly correlated with the diagnosis of uterine sarcoma in our population.

If we consider the performance of each individual feature, DWI showed the best accuracy (87%), with significant correlation ($p < 0.01$). All uterine sarcomas in our population showed restricted diffusion: DWI showed to have a sensibility of 100% with no false-negative (FN) cases and a high NPV. Based on literature data, previously proposed ADC values threshold ranged from 0.8 to $1.2 \times 10^{-3} \text{ mm}^2/\text{s}$ [27], in our cohort overall accuracy reached its maximum value

for an ADC value threshold of $0.903 \times 10^{-3} \text{ mm}^2/\text{s}$ (Youden index = 0.84).

On the other hand, 7/41 leiomyoma showed a restricted diffusion (1 typical leiomyoma with areas of hyaline degeneration, 2 myxoid degenerated leiomyoma, 3 cellular leiomyoma and 1 leiomyoma with bizarre nuclei): The major limit of the mono-parametric approach (evaluation of DWI alone) is the lower specificity.

During the evaluation of DWI and especially of ADC map, it is important to avoid some pitfalls due to the presence of blood products; this type of misinterpretation (false restricted DWI) involves especially less experienced readers.

It is mandatory to correlate DWI signal with both T2 and T1 signal to not interpret hemorrhagic foci (T1 hyperintense), necrotic areas (without CE even in the late phase) or cystic areas (T2-hyperintensity, T1-hypointense both before and after contrast) as area of real restricted signal, which are hypointense on T2 and T1 wi.

Also, ADC map quantitative evaluation had some pitfalls. In our cohort, leiomyomas ADC map values were strongly heterogeneous ranging from 0.64 to $2.55 \times 10^{-3} \text{ mm}^2 \text{ s}^{-1}$.

Some of the lowest ADC value were detected in homogeneous strongly T2 hypointense lesion due to the T2 *black out* effect. These cases didn't show a real restricted diffusion because they were hypointense both on DWI and ADC. This finding highlighted the importance of prior visual assessment of DWI signal and secondly quantitative assessment especially in doubt cases.

Among the different single imaging features, T1 SI and enhancement type (heterogeneous and during early phase) with central areas of necrosis revealed to be the most specific (specificity 87.8%) but both showed a very low sensibility 69.23% and 53.85%, respectively.

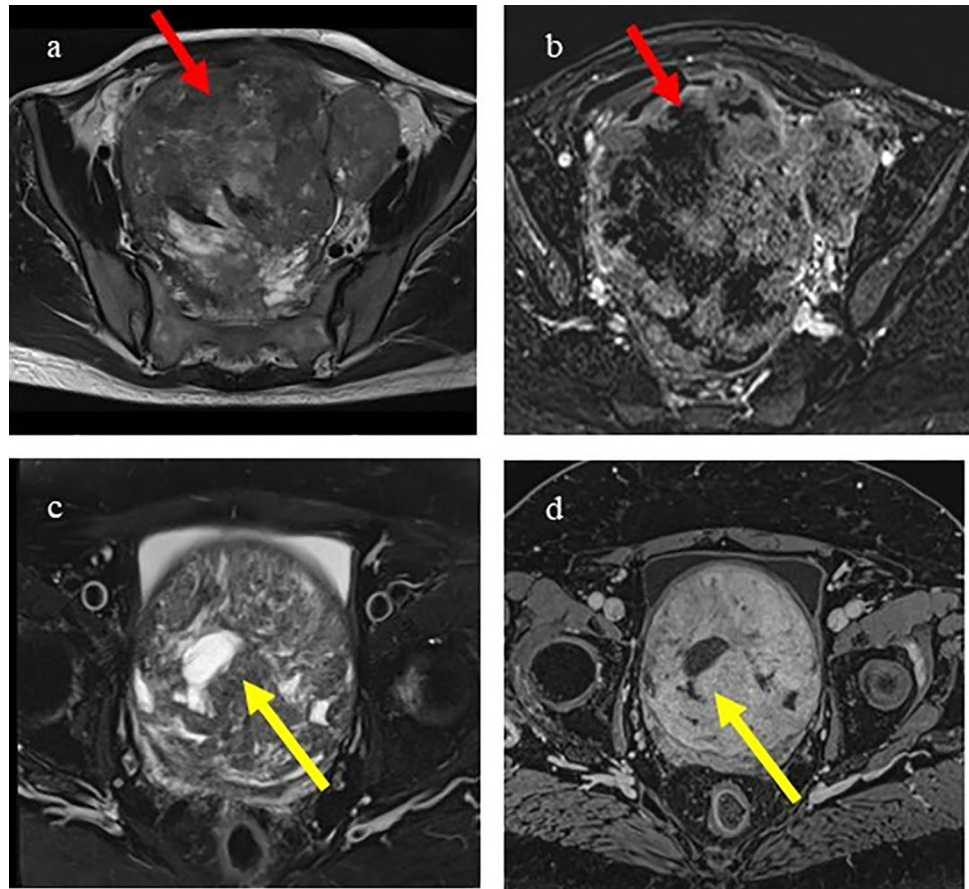
In this context, a potential pitfall is to consider all avascular areas as necrotic due to the lack of contrast enhancement. It is important to differentiate real tumoral necrosis from areas of cystic or red degeneration because their pathogenesis is very different: Red degeneration is the consequence of a venous infarction and represent a coagulative necrosis, while avascular areas in a sarcomatous tissue is due to hemorrhagic tumoral necrosis [15].

In the evaluation of the presence of necrotic area, it is mandatory to evaluate also T2 signal intensity for distinguishing between necrotic areas (T2 hypointense/intermediate signal) and areas of hyaline, cystic or red cell degeneration, also avascular, but with different T2 signal intensity (Fig. 7).

The integration of signal information derived from all MR sequences resulted essential to proper analyze imaging characteristic of the lesion and to reach the adequate diagnosis.

Therefore, our results confirmed the importance of a multiparametric approach in MR interpretation.

Fig. 7 Uterine leiomyosarcoma characterized by internal areas of T2 intermediate signal **a**, central avascular on post-contrast T1FS WI with irregular margins **b**, typical for internal neoplastic necrosis (red arrow in **a** and **b**). The lesion in **c** and **d** showed internal well-defined area of T2 hyperintense signal **c**, avascular on T1 FS WI **d**, suggestive for leiomyoma with cystic degeneration (arrow in **c** and **d**)



In the presence of three imaging features favoring malignancy, MRI obtained the best diagnostic performance in terms of accuracy (94.44%), and specificity (97.56%).

The aim of our work was to develop a diagnostic algorithm and a scoring system able to differentiate uterine leiomyoma and sarcoma.

The importance of using a standard approach in the interpretation of MRI features and the need of a real radiological grading system, such as BI-RADS or PI-RADS, to stratify patients with uterine masses, result more and more evident, as recently highlighted by Tong et al. [26].

A risk grading system is essential to standardize lexicon, to guide less experienced radiologists to proper diagnosis and to improve communication with gynecologists, minimizing confusion in the interpretation of radiological reports and consequent mismanagement.

Our proposed algorithm allowed to improve both JR and SR performance (algorithm-aided accuracy 88.46% and 96%, respectively) and determined a significant increase in inter-observer agreement (Cohen's k : 0.847 between SR and JR's algorithm-aided report) helping even the less-experienced radiologist in this difficult differential diagnosis.

Moreover, we appreciated a further performance improvement thanks to the evaluation of ancillary features (morphological and clinical ones) in doubt cases that reduced the number of FN case, increasing especially sensibility (Table 3).

One lesion (1 LG-ESS) was initially classified with score 3 by both readers but, considering the “ancillary features” (in this case the presence of irregular margins), it can be correctly re-classified as score 4. The misinterpretation of LG-ESS can reflect its distinct biological behavior and clinical outcome: although LG-ESS can show extra-uterine involvement, metastasis, and recurrence, it is considered as relatively indolent lesion compared to the other uterine sarcomas (especially LMS, HG ESS and UES) associated with long term survival.

We know that in this clinical scenario the specificity is less important than sensibility due to the rarity of these tumors but the presence of 4 or more features favoring malignancy (score 5) demonstrated a high specificity (100%) with no false positive (FP) case.

These are diagnosis that we can't miss: in the evaluation of a uterine mass with these imaging features (score 5) the suspect of sarcoma is high and must be promptly and correctly communicated to the referring clinician (Fig. 8).

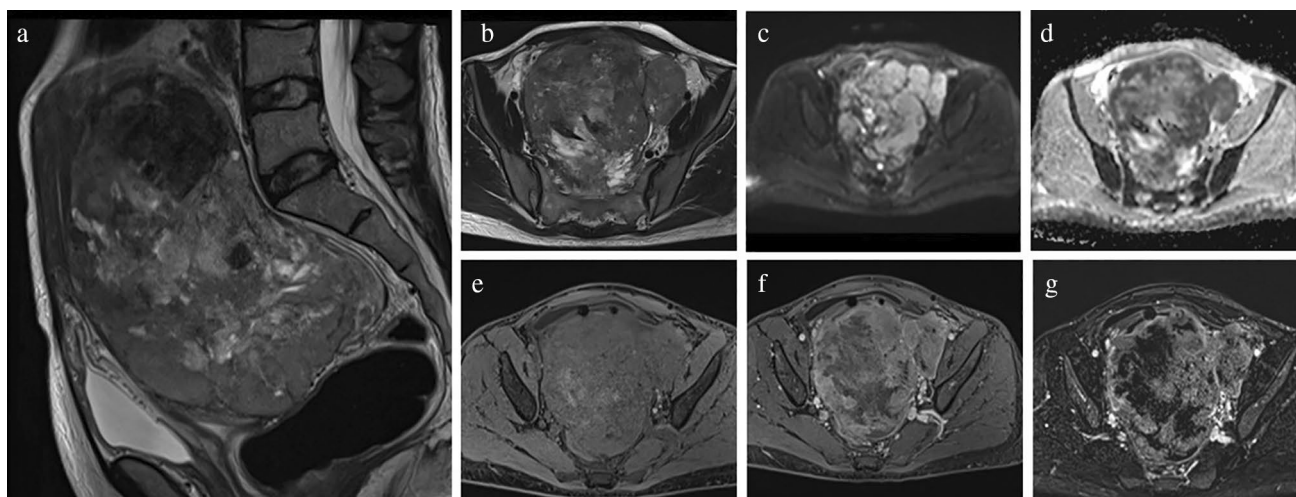


Fig. 8 Uterine leiomyosarcoma: MRI showed large uterine mass characterized by heterogeneous and intermediate signal on T2 (**a** coronal, **b** axial plane), significant restriction of diffusion (strongly hyperintensity on DWI and strongly hypointensity on ADC map),

some intralesional hemorrhagic foci on T1WI **c** and early contrast enhancement (**f**, T1WI arterial phase after contrast) with central areas of necrosis (**g**, venous phase)

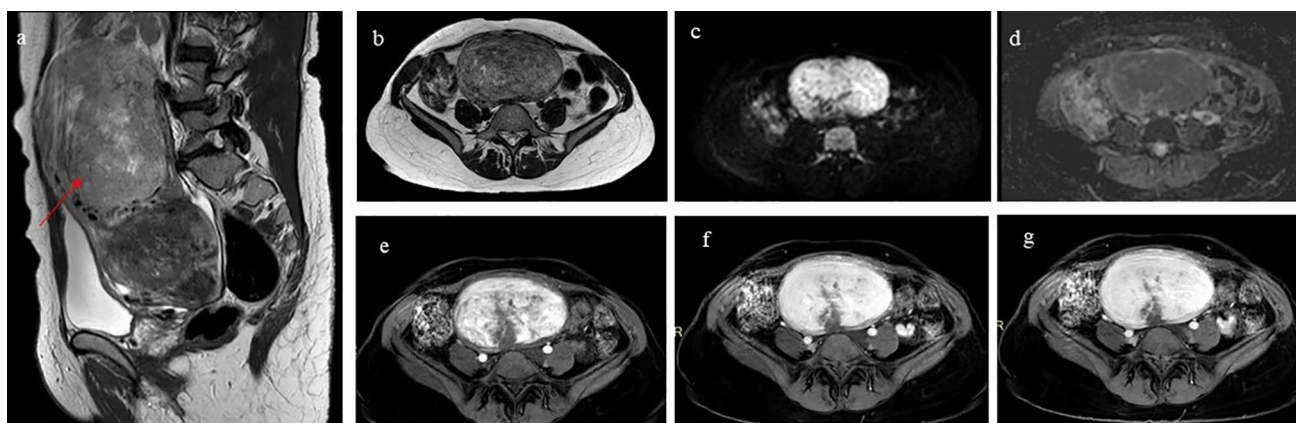


Fig. 9 A rapid uterine growth mass in a post-menopausal woman revealed to be a leiomyoma with bizarre nuclei. Sagittal **a** and axial **b** T2WI demonstrated a large heterogeneous uterine mass (red arrow in A) that showed diffusion restriction with high signal intensity on

DWI **c** and hypointensity on ADC map **d**. There were some internal avascular areas with intermediate T2- signal compatible with focal internal necrosis. No internal hemorrhagic foci were present

In the elaboration of our algorithm, we decided to start with DWI signal evaluation due to its high NPV. For the same reason, on the second step, we decided to evaluate T2 signal.

In case of no restricted DWI and T2 homogeneous hypointense signal, the examined lesion has a real low risk to be malignant due to the high NPV of these two MR parameters.

Presently, based on literature data, we were not able to completely rule out the diagnosis of uterine sarcoma in case of a mass with no restricted diffusion and with an heterogeneous intermediate T2 signal. In these cases, also other MR features must be considered, and, in case

of doubt, clinical data and a multidisciplinary discussion are mandatory.

The diagnostic algorithm proposed was independent of the presence of ascites, pelvic peritoneal or extraperitoneal implants, pelvic lymphadenomegalies that are clear signs of malignancy but not specific for uterine sarcoma due to its preferential hematogenous spread. In these cases, it is necessary to consider also other differential diagnosis.

In our cohort, algorithm both SR and JR sensibility was 100% but we are aware that further validation studies are needed. Specificity was for, respectively, 93,33% SR and for 78.57% for JR.

Both reader (SR and JR) indicated as score 4 a case of atypical subtype of leiomyoma (leiomyoma with bizarre nuclei) that presented as a rapid uterine growth mass in a post-menopausal woman, as shown in Fig. 9. This was a very rare subtype of leiomyoma that represented a real diagnostic challenge and highlighted the problem of possible overlap of imaging features between benign and malignant lesion.

In the context of such rare pathologies with a very poor prognosis is always important to remember that, in doubtful cases, multidisciplinary approach is necessary to a proper risk–benefit analysis (over-treatment versus underestimate).

Moreover, the JR erroneously classified two benign lesions (1 myxoid degenerated and 1 a red degenerated leiomyoma) with score 4 due to misinterpretation of SI.

Especially unexperienced radiologists must remember some important artifacts/pitfalls to not erroneously describe the SI of a lesion (Table 2):

In DWI signal evaluation, radiologists must be familiar with T2-*shine through* and T2 *blackout effect* and avoid in the quantitative assessment on ADC map the hemorrhagic foci (T1 hyperintense), necrotic areas (without CE even in the late phase) or cystic areas (T2-hyperintensity, T1-hypointense both before and after contrast), Fig. 10.

Our preliminary results showed how the application of the algorithm improved the performance of both the JR and SR with a significant increase in sensitivity, specificity and accuracy.

Moreover, the algorithm showed a better performance than simply evaluation of co-presence of 3 or more MR signals features.

The application of the diagnostic algorithm allowed a proper identification of suspicious features with an easy and systematic approach.

Furthermore, diagnostic algorithm and standard lexicon application induced a significant increase in the inter-observer agreement with a better risk stratification of these patient.

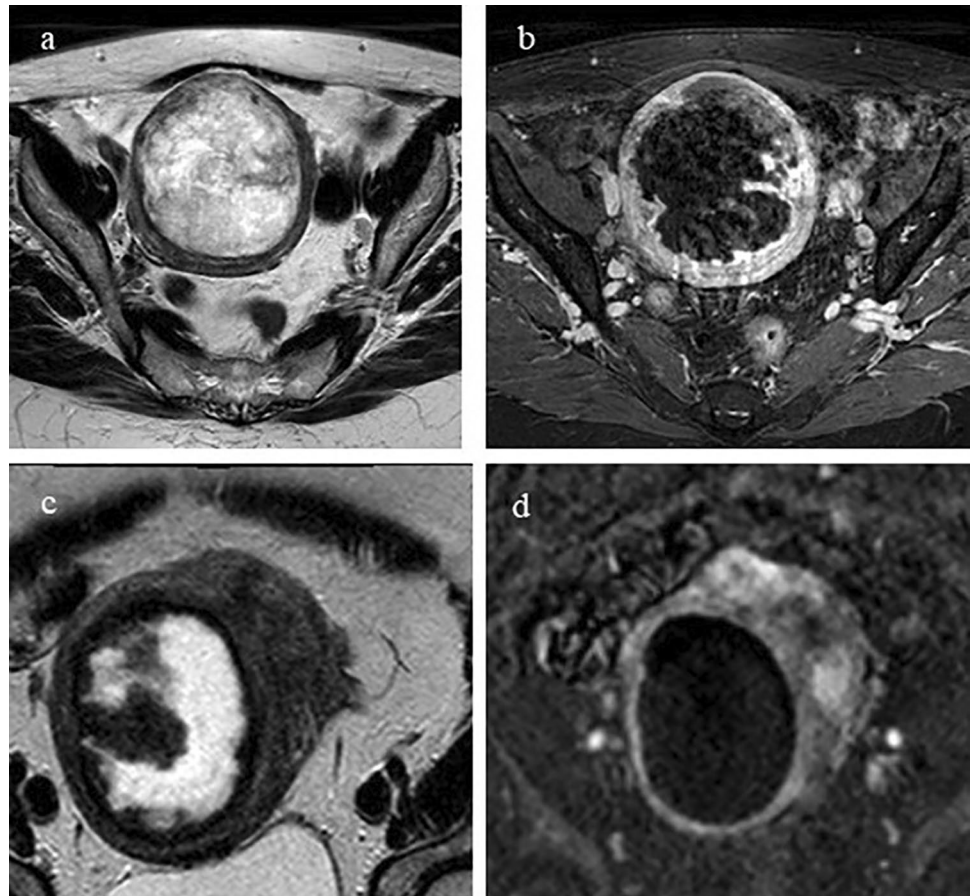
Our study had several limitations.

Firstly, the number of patients was relatively small due to the rarity of the disease.

Secondly, it was a retrospective study and further external and prospective validation with a larger patient cohort is needed. External validation is an important step in the validation of a diagnostic algorithm and score system to avoid overfitting to the training dataset, potentially resulting in an overestimation of the algorithm diagnostic performance.

Finally, it was a multicentric study and included images from multiple MRI scanners without a uniform protocol.

Fig. 10 Difference between tumoral necrosis (a T2WI, b T1WI after contrast) and benign red degeneration (c T2WI, d T1WI after contrast): tumoral necrosis showed inner irregular margins while red degenerated leiomyoma showed complete avascularity with a regular internal profile



On the other hand, this aspect can better reflect the typical clinical practice. Indeed, most of our examination was performed with a multiphasic acquisition, but dynamic contrast enhancement acquisition is presently encouraged and considered by ESUR as the optimal technique for better assessment of areas of early enhancement and of necrosis [12].

Conclusion

Uterine leiomyomas and sarcomas frequently show an overlap of clinical and imaging features, especially in the presence of degenerate and large leiomyomas.

Furthermore, considering the low prevalence of uterine malignant mesenchymal tumors compared to common leiomyomatous lesions, the risk of underestimating a myometrial mass is significant, with important clinical and therapeutic consequences.

Our proposed algorithm improved the performance of both the JR and SR with a significant increase in sensitivity, specificity, and accuracy.

In the diagnostic evaluation of MRI features, the use of a diagnostic algorithm can help the radiologist, even the less experienced ones, to standardize the approach to a complex myometrial mass and more easily identify suspicious features.

However, it should be always remembered that the result obtained from image interpretation represents only a probability of the risk of malignancy and, in unclear cases, a multidisciplinary approach is mandatory to properly manage these patients.

Supplementary Information The online version contains supplementary material available at <https://doi.org/10.1007/s11547-023-01654-1>.

Author contributions All authors contributed to the study conception and design. Material preparation, data collection and analysis were performed by Rosa Francesca and Martinetti Carola. The first draft of the manuscript was written by Rosa Francesca and Martinetti Carola, and all authors commented on previous versions of the manuscript. All authors read and approved the final manuscript.

Funding The authors declare that no funds, grants, or other support were received during the preparation of this manuscript.

Declarations

Conflict of interest The authors have no relevant financial or non-financial interests to disclose.

Ethics approval This non-interventional, observational, and retrospective study was approved by the Internal Review Board of the Diagnostic Imaging Department and by the Regional Ethics Committee (N. CER Liguria: 78/2023-DB id 12833).

Consent to participate Informed consent was obtained from all individual participants included in the study.

References


- Pavone D, Clemenza S, Sorbi F, Fambrini M, Petraglia F (2018) Epidemiology and risk factors of uterine fibroids. *Best Pract Res Clin Obstet Gynaecol* 46:3–11. <https://doi.org/10.1016/j.bpobgyn.2017.09.004>. (Epub 2017 Oct 1 PMID: 29054502)
- Parker WH (2007) Etiology, symptomatology, and diagnosis of uterine myomas. *Fertil Steril* 87(4):725–736. <https://doi.org/10.1016/j.fertnstert.2007.01.093>. (PMID: 17430732)
- Memarzadeh S, Berek J (2019) Uterine sarcoma: classification, epidemiology, clinical manifestations, and diagnosis. UpToDate. Accessed 28 June 2021
- Koivisto-Korander R, Butzow R, Koivisto AM, Leminen A (2008) Clinical outcome and prognostic factors in 100 cases of uterine sarcoma: experience in Helsinki University Central Hospital 1990–2001. *Gynecol Oncol* 111(1):74–81. <https://doi.org/10.1016/j.ygyno.2008.06.002>. (Epub 2008 Jul 26 PMID: 18657852)
- Kim K. et al. Tumors of the uterine corpus. In: WHO classification of tumors: female genital tumours, 5th edn, pp 245–308
- Ferrandina G, Aristei C, Biondetti PR, Cananzi FCM, Casali P, Ciccarone F, Colombo N, Comandone A, Corvo' R, De Iaco P, Dei Tos AP, Donato V, Fiore M, Franchi GA, Gronchi A, Guerriero S, Infante A, Odicino F, Pirroni T, Quagliuolo V, Sanfilippo R, Testa AC, Zannoni GF, Scambia G, Lorusso D (2020) Italian consensus conference on management of uterine sarcomas on behalf of S.I.G.O. (Societa' italiana di Ginecologia E Ostetricia). *Eur J Cancer* 139:149–168. <https://doi.org/10.1016/j.ejca.2020.08.016>. (Epub 2020 Sep 29. Erratum in: *Eur J Cancer*. 2021 Feb;144:397-398. PMID: 32992154)
- US Food and Drug Administration. Laparoscopic power morcellation during uterine surgery for fibroids. "Meeting of FDA's obstetrics and gynecology devices panel of the Medical Devices Advisory Committee." FDA Executive Summary, 2014, pp. 18–24, <https://wayback.archive-it.org/7993/20170113091521/http://www.fda.gov/downloads/AdvisoryCommittees/CommitteesMeetingMaterials/MedicalDevices/MedicalDevicesAdvisoryCommittee/ObstetricsandGynecologyDevices/UCM404148.pdf>. Accessed 3 Mar 2022
- Suzuki A, Aoki M, Miyagawa C, Murakami K, Takaya H, Kotani Y, Nakai H, Matsumura N (2019) Differential diagnosis of uterine leiomyoma and uterine sarcoma using magnetic resonance images: a literature review. *Healthcare (Basel)* 7(4):158. <https://doi.org/10.3390/healthcare7040158>. PMID: 31817500; PMCID: PMC6955943
- Munro MG, Critchley HO, Broder MS, Fraser IS, FIGO Working Group on Menstrual Disorders (2011) FIGO classification system (PALM-COEIN) for causes of abnormal uterine bleeding in nongravid women of reproductive age. *Int J Gynaecol Obstet* 113(1):3–13. <https://doi.org/10.1016/j.ijgo.2010.11.011>. (Epub 2011 Feb 22. PMID: 21345435)
- Porter AE, Kho KA, Gwin K (2019) Mass lesions of the myometrium: interpretation and management of unexpected pathology. *Curr Opin Obstet Gynecol* 31(5):349–355. <https://doi.org/10.1097/GCO.0000000000000569>. (PMID: 31425175)
- Lin G, Yang LY, Huang YT, Ng KK, Ng SH, Ueng SH, Chao A, Yen TC, Chang TC, Lai CH (2016) Comparison of the diagnostic accuracy of contrast-enhanced MRI and diffusion-weighted MRI in the differentiation between uterine leiomyosarcoma/smooth muscle tumor with uncertain malignant potential and benign leiomyoma. *J Magn Reson Imaging* 43(2):333–342. <https://doi.org/10.1002/jmri.24998>. (Epub 2015 Sep 18 PMID: 26383110)
- Kubik-Huch RA, Weston M, Nougaret S, Leonhardt H, Thomassin-Naggara I, Horta M, Cunha TM, Maciel C, Rockall A, Forstner R (2018) European Society of Urogenital Radiology (ESUR) guidelines: MR imaging of leiomyomas. *Eur Radiol*

- 28(8):3125–3137. <https://doi.org/10.1007/s00330-017-5157-5>. (Epub 2018 Feb 28. PMID: 2942599; PMCID: PMC6028852)
13. Lakhman Y, Veeraraghavan H, Chaim J, Feier D, Goldman DA, Moskowitz CS, Nougaret S, Sosa RE, Vargas HA, Soslow RA, Abu-Rustum NR, Hricak H, Sala E (2017) Differentiation of uterine leiomyosarcoma from atypical leiomyoma: diagnostic accuracy of qualitative MR imaging features and feasibility of texture analysis. *Eur Radiol* 27(7):2903–2915. <https://doi.org/10.1007/s00330-016-4623-9>. (Epub 2016 Dec 5. PMID: 27921159; PMCID: PMC5459669)
 14. Bi Q, Xiao Z, Lv F, Liu Y, Zou C, Shen Y (2018) Utility of clinical parameters and multiparametric MRI as predictive factors for differentiating uterine sarcoma from atypical leiomyoma. *Acad Radiol* 25(8):993–1002. <https://doi.org/10.1016/j.acra.2018.01.002>. (Epub 2018 Feb 13 PMID: 29422425)
 15. Nakai G, Yamada T, Hamada T, Atsukawa N, Tanaka Y, Yamamoto K, Higashiyama A, Juri H, Nakamoto A, Yamamoto K, Hirose Y, Ohmichi M, Narumi Y (2017) Pathological findings of uterine tumors preoperatively diagnosed as red degeneration of leiomyoma by MRI. *Abdom Radiol (NY)* 42(7):1825–1831. <https://doi.org/10.1007/s00261-017-1126-3>. PMID: 28389786; PMCID: PMC5486831
 16. Abdel Wahab C, Jannot AS, Bonaffini PA, Bourillon C, Cornou C, Lefrère-Belda MA, Bats AS, Thomassin-Naggara I, Bellucci A, Reinhold C, Fournier LS (2020) Diagnostic algorithm to differentiate benign atypical leiomyomas from malignant uterine sarcomas with diffusion-weighted MRI. *Radiology* 297(3):E347. [https://doi.org/10.1148/radiol.202009020.Erratumfor:Radiology.2020Nov;297\(2\):361-371](https://doi.org/10.1148/radiol.202009020.Erratumfor:Radiology.2020Nov;297(2):361-371). (PMID: 33196375)
 17. Tamai K, Koyama T, Saga T, Morisawa N, Fujimoto K, Mikami Y, Togashi K (2008) The utility of diffusion-weighted MR imaging for differentiating uterine sarcomas from benign leiomyomas. *Eur Radiol* 18(4):723–730. <https://doi.org/10.1007/s00330-007-0787-7>. (Epub 2007 Oct 10 PMID: 17929022)
 18. Brooks SE, Zhan M, Cote T, Baquet CR (2004) Surveillance, epidemiology, and end results analysis of 2677 cases of uterine sarcoma 1989–1999. *Gynecol Oncol* 93(1):204–208. <https://doi.org/10.1016/j.ygyno.2003.12.029>. (PMID: 15047237)
 19. Namimoto T, Yamashita Y, Awai K, Nakaura T, Yanaga Y, Hirai T, Saito T, Katabuchi H (2009) Combined use of T2-weighted and diffusion-weighted 3-T MR imaging for differentiating uterine sarcomas from benign leiomyomas. *Eur Radiol* 19(11):2756–2764. <https://doi.org/10.1007/s00330-009-1471-x>. (Epub 2009 Jun 6 PMID: 19504102)
 20. Thomassin-Naggara I, Dechoux S, Bonneau C, Morel A, Rouzier R, Carette MF, Darai E, Bazot M (2013) How to differentiate benign from malignant myometrial tumours using MR imaging. *Eur Radiol* 23(8):2306–2314. <https://doi.org/10.1007/s00330-013-2819-9>. (Epub 2013 Apr 8 PMID: 23563602)
 21. Kaganov H, Ades A, Fraser DS (2018) Preoperative magnetic resonance imaging diagnostic features of uterine leiomyosarcomas: a systematic review. *Int J Technol Assess Health Care* 34(2):172–179. <https://doi.org/10.1017/S0266462318000168>. (Epub 2018 Apr 12 PMID: 29642961)
 22. Nagai T, Takai Y, Akahori T, Ishida H, Hanaoka T, Uotani T, Sato S, Matsunaga S, Baba K, Seki H (2014) Novel uterine sarcoma preoperative diagnosis score predicts the need for surgery in patients presenting with a uterine mass. *Springerplus* 18(3):678. <https://doi.org/10.1186/2193-1801-3-678>. PMID: 25520907; PMCID: PMC4247829
 23. Sun S, Bonaffini PA, Nougaret S, Fournier L, Dohan A, Chong J, Smith J, Addley H, Reinhold C (2019) How to differentiate uterine leiomyosarcoma from leiomyoma with imaging. *Diagn Interv Imaging* 100(10):619–634. <https://doi.org/10.1016/j.diii.2019.07.007>. (Epub 2019 Aug 16 PMID: 31427216)
 24. Smith J, Zawaideh JP, Sahin H, Freeman S, Bolton H, Addley HC (2021) Differentiating uterine sarcoma from leiomyoma: BET-1T2ER Check! *Br J Radiol* 94(1125):20201332. <https://doi.org/10.1259/bjr.20201332>. (Epub 2021 May 5. PMID: 33684303; PMCID: PMC9327746)
 25. Tong A, Kang SK, Huang C, Huang K, Slevin A, Hindman N (2019) MRI screening for uterine leiomyosarcoma. *J Magn Reson Imaging* 49(7):e282–e294. <https://doi.org/10.1002/jmri.26630>. (Epub 2019 Jan 13 PMID: 30637854)
 26. Hindman N, Kang S, Fournier L, Lakhman Y, Nougaret S, Reinhold C, Sadowski E, Huang JQ, Ascher S (2022) MRI evaluation of uterine masses for risk of leiomyosarcoma: a consensus statement. *Radiology*. <https://doi.org/10.1148/radiol.211658>. (Epub ahead of print. PMID: 36194109)
 27. Héléage S, Vandeventer S, Buy JN, Bordonné C, Just PA, Jacob D, Ghossain M, Rousset P, Dion É (2021) Uterine sarcomas: are there MRI signs predictive of histopathological diagnosis? A 50-patient case series with pathological correlation. *Sarcoma* 1(2021):8880080. <https://doi.org/10.1155/2021/8880080>. (PMID: 34305438)

Publisher's Note Springer Nature remains neutral with regard to jurisdictional claims in published maps and institutional affiliations.

Springer Nature or its licensor (e.g. a society or other partner) holds exclusive rights to this article under a publishing agreement with the author(s) or other rightsholder(s); author self-archiving of the accepted manuscript version of this article is solely governed by the terms of such publishing agreement and applicable law.

Authors and Affiliations

Francesca Rosa¹  · Carola Martinetti² · Silvia Magnaldi³ · Stefania Rizzo^{4,5} · Lucia Manganaro⁶ · Stefania Migone² · Silvia Ardoino⁷ · Daria Schettini² · Pierangelo Marchiolè^{8,9} · Tommaso Ragusa¹⁰ · Nicoletta Gandolfo²

✉ Francesca Rosa
francescarosa892@gmail.com

Carola Martinetti
carola.martinetti@asl3.liguria.it

Silvia Magnaldi
simagn@tin.it

Stefania Rizzo
stefaniamariarita.rizzo@eoc.ch

Lucia Manganaro
lucia.manganaro@uniroma1.it

Stefania Migone
stefania.migone@asl3.liguria.it

Silvia Ardoino
s.ardoino@asl2.liguria.it

Daria Schettini
daria.schettini@asl3.liguria.it

Pierangelo Marchiolè
pierangelo.marchiole@hsanmartino.it

Tommaso Ragusa
tommaso.ragusa@asl3.liguria.it

Nicoletta Gandolfo
nicoletta.gandolfo@asl3.liguria.it

- ¹ Diagnostic Imaging Department, San Paolo Hospital-ASL 2, via Genova, 30, Savona, Italy
- ² Diagnostic Imaging Department, Villa Scassi Hospital-ASL 3, Corso Scassi 1, Genoa, Italy
- ³ Diagnostic Imaging Unit, Esperia Medical Center, Porcia, PN, Italy
- ⁴ Service of Radiology, Imaging Institute of Southern Switzerland, Clinica di Radiologia EOC, 6900 Lugano, Switzerland

- ⁵ Faculty of Biomedical Sciences, Università della Svizzera Italiana (USI), via Buffi 23, 6900 Lugano, Switzerland
- ⁶ Department of Radiological, Oncological and Pathological Sciences, Sapienza University of Rome, 00185 Rome, Italy
- ⁷ Anatomic Pathology Unit, San Paolo Hospital-ASL 2, via Genova, 30, Savona, Italy
- ⁸ Obstetrics and Gynecology Unit, Villa Scassi Hospital-ASL 3, Corso Scassi 1, Genoa, Italy
- ⁹ Obstetrics and Gynecology Department, IRCCS ospedale Policlinico San Martino, Genoa, Italy
- ¹⁰ Anatomic Pathology Unit, Villa Scassi Hospital-ASL 3, Corso Scassi 1, Genoa, Italy